ACS APPLIED MATERIALS & INTERFACES

Research Article

www.acsami.org

Functionalized Carbon Nanotube via Distillation Precipitation Polymerization and Its Application in Nafion-Based Composite Membranes

Guangwei He,[†,‡] Jing Zhao,[†,‡] Shen Hu,[†] Lingqiao Li,[†] Zongyu Li,[†,‡] Yifan Li,[†,‡] Zhen Li,[†,‡] Hong Wu,[†,‡] Xinlin Yang,[‡,§] and Zhongyi Jiang*[,†,‡]

[†]Key Laboratory for Green Chemical Technology of Ministry of Education, School of Chemical Engineering and Technology, Tianjin University, Tianjin 300072, China

[‡]Collaborative Innovation Center of Chemical Science and Engineering (Tianjin), Tianjin 300072, China

[§]Key Laboratory of Functional Polymer Materials, Ministry of Education, Institute of Polymer Chemistry, Nankai University, Tianjin 300071, China

Supporting Information

ABSTRACT: The objective of this study is to develop a novel approach to *in situ* functionalizing multiwalled carbon nanotubes (MWCNTs) and exploring their application in Nafion-based composite membranes for efficient proton conduction. Covalent grafting of acrylate-modified MWCNTs with poly(methacrylic acid-*co*-ethylene glycol dimethacrylate), poly(vinylphosphonic acid-*co*-ethylene glycol dimethacrylate), and sulfonated poly(styrene-*co*-divinylbenzene) was achieved via surface-initiated distillation precipitation polymerization. The formation of core−shell structure was verified by TEM images, and polymer layers with thickness around 30 nm were uniformly covered on the MWCNTs. The graft yield reached up to 93.3 wt % after 80 min of polymerization. The functionalized CNTs (FCNTs) were incorporated into the Nafion matrix to prepare composite membranes. The influence of various functional groups (−COOH, $-PO_3H_2$, and $-SO_3H$) in FCNTs on proton transport of the composite membranes was studied. The incorporation of FCNTs afforded the composite membranes significantly enhanced proton conductivities under reduced relative humidity. The composite membrane containing 5 wt % phosphorylated MWCNTs (PCNTs) showed the highest proton conductivity, which was attributed to the construction of lower-energy-barrier proton transport pathways by PCNTs, and excellent water-retention and proton-conduction properties of the cross-linked polymer in PCNTs. Moreover, the composite membranes exhibited an enhanced mechanical stability.

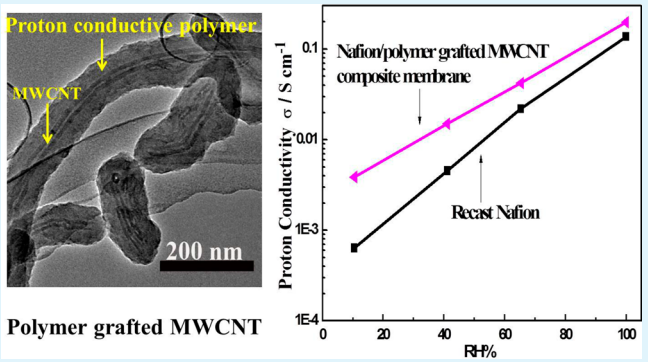

KEYWORDS: *carbon nanotubes, distillation−precipitation−polymerization, Nafion, composite membranes, proton conductivity under low humidity, mechanical properties*

1. INTRODUCTION

Recently, carbon nanotubes (CNTs) have attracted enormous research efforts due to their unique combinations of various chemical and physical properties such as electrical and thermal conductivity, optical properties, and high mechanical stability.[1−4] However, CNTs are insoluble in almost all solvents because of strong van der Waals interactions that tightly hold them together, forming bundles and ropes. This aggregation behavior restricts their processability and impairs their performance at the nanoscale level.[1,5] To address these problems, a myriad of approaches to functionalizing CNTs have been developed including surfactant modification, polymer absorption, end-group reactions to covalently graft micromolecule or polymer.[6−9] Among these approaches, covalent functionalization of CNTs with high-molecular-weight polymers is of great advantage because the properties of the CNTs can be adjusted via polymer modification to meet broader application requirements and be more compatible with a target matrix.[5,10−12] The covalent functionalization consists of "grafting to" and "grafting from" strategies.[11] The "grafting to" method refers to the chemical bonding of end-functionalized polymers to the reactive surface of CNTs. The "grafting from" method refers to the *in situ* generating polymer on the initiator-tethered surface of CNTs. Compared with "grafting to" strategies, "grafting from" strategies allow high-molecular-weight polymers to be efficiently generated on the CNTs

Received: June 13, 2014
Accepted: August 10, 2014
Published: August 10, 2014

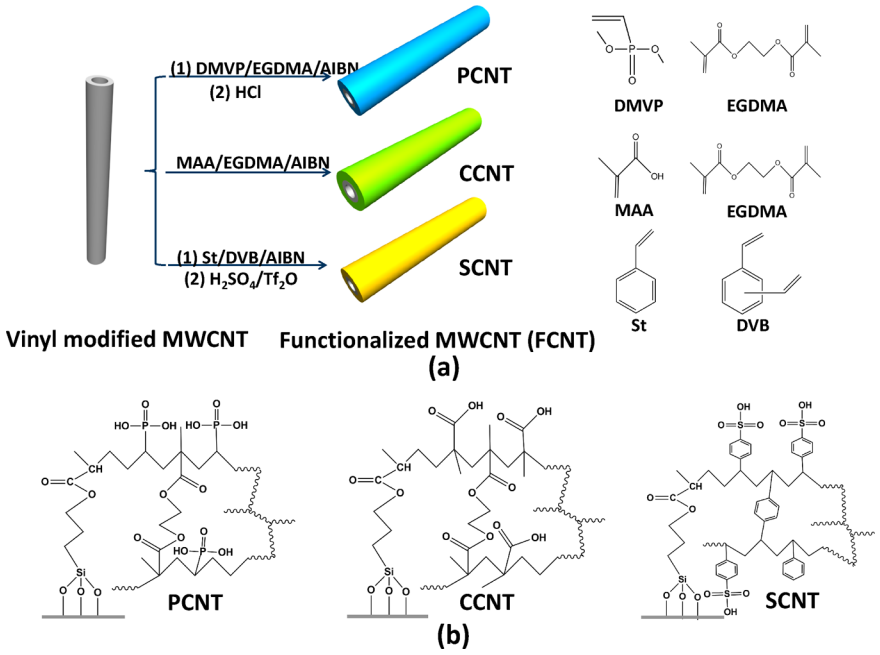

Figure 1. Schematic illustration for (a) the synthesis and (b) the structure of functionalized MWCNTs.

without the severe limitation of steric hindrance. Various "grafting from" polymerization approaches such as atom transfer radical polymerization (ATRP),[13] reversible addition−fragmentation chain transfer,[14] and emulsion polymerization[15] have been widely employed to *in situ* generate polymers on CNTs. Herein, we report the functionalization of multiwalled carbon nanotubes (MWCNTs) via distillation−precipitation−polymerization for the first time. Distillation−precipitation−polymerization is chosen primarily because of its distinct ability to form a cross-linked polymer shell with well-controlled thickness on a vinyl modified surface as well as its simplicity and high efficiency.[16−18]

Nafion is one of the most promising state-of-the-art proton exchange membranes (PEMs) due to its high proton conductivity under hydrated humidity and excellent chemical and mechanical durability.[19−21] However, Nafion suffers from a severe limitation that it dehydrates under low relative humidity (RH, < 50%), leading to a significant decline of proton conductivity.[22] For enhancing proton conductivity under a RH of 100%, dispersion of acid-modified CNTs into Nafion matrix has been demonstrated as a feasible avenue because it is capable of rendering the membrane continuous pathways for facile proton transport.[6,23−26] Pillai et al. reported that 0.05 wt % of sulfonated single-walled CNTs (S-SWCNT) significantly enhanced the proton conductivity of Nafion-based membranes at 60 °C from 0.09 to 0.56 S cm^{-1} (522% increace, under 100% RH) and proposed that S-SWCNTs helped the formation of better channel-like networks for proton transport.[24] However, the proton conductivity under low RH is yet to be explored. The good water retention property of PEM plays a crucial role in the formation of percolated water domains for facile proton transport under low RH.[27] Highly cross-linked hydrophilic polymer structures have been proven efficient in retaining water due to their ability of bonding water via hydrophilic interactions (hydrogen or electrostatic bonds) and capillary force.[28−30] Thus, it can be envisioned that proton conductivity of Nafion under low RH can be enhanced if CNTs grafted with cross-linked hydrophilic polymer are incorporated into Nafion.

In this study, MWCNTs were functionalized with three types of cross-linked polymers (poly(methacrylic acid-*co*-ethylene glycol dimethacrylate), poly(vinylphosphonic acid-*co*-ethylene glycol dimethacrylate), and sulfonated poly(styrene-*co*-divinylbenzene)) via distillation−precipitation−polymerization (Figure 1) and incorporated into Nafion. The functionalized MWCNTs (FCNTs) were characterized by transmission electron microscopy (TEM), Fourier transform infrared spectroscopy (FTIR), thermogravimetric analysis (TGA), and Zeta PALS. The influence of various functional groups (−COOH, $-PO_3H_2$, and $-SO_3H$) in FCNTs on proton transport was studied. Moreover, the mechanical properties of the composite membranes were investigated.

2. EXPERIMENTAL PROCEDURES

2.1. Materials. Hydroxylated MWCNTs (outside diameter, 10−20 nm; length, 0.5−2 μm; −OH content, 3.06 wt %) were purchased from XF NANO, Inc. (Nanjing, China). Nafion solution (5 wt %, DE520) and Nafion 117 was provided by Dupont. 3-(Methacryloxy)-propyltrimethoxysilane (MPS), ethylene glycol dimethacrylate (EGDMA), dimethylvinylphosphonate (DMVP), divinylbenzene (DVB, 80% divinylbenzene isomers), and styrene (St) were purchased from Alfa Aesar and used as received. 2,2′-Azoisobutyronitrile (AIBN) was purchased from Aladdin (China) and used without further purification. Methacrylic acid (MAA) (Tianjin Guangfu Fine Chemical Engineering Institute) was purified by vacuum distillation. Acetonitrile was dehydrated over calcium hydride and distilled. All other reagents were of reagent grade and used without further purification. Deionized water was utilized in the entire experiment.

2.2. Grafting Cross-Linked Polymer onto MWCNTs. MWCNTs were modified with MPS to introduce vinyl groups as grafting sites for the following polymer growth. Briefly, 0.5 g of MWCNTs and 50 mL of ethanol were mixed under ultrasonic irradiation, and 0.5 mL of MPS was added into the above solution. Then, the solution was stirred for 48 h at 50 °C, and the MPS modified MWCNTs (MPS-CNTs) were gathered by centrifugation and two dispersion/centrifugation cycles using ethanol as solvent. Finally, the MPS-CNTs black powder was obtained by drying under vacuum at 80 °C for 24 h.

The grafting of polymer on the MPS-CNTs was achieved by surface-initiated precipitation polymerization.[16,18] The grafting of

poly(DMVP-*co*-EGDMA) on MPS-CNTs was described as follows. In a 100 mL flask, 0.04 g of MPS-CNTs was dispersed in 80 mL of acetonitrile with assistance of ultrasonic irradiation. A fractionating column, Liebig condenser, and receiver were attached to the flask to condense and collect the solvent. The initiator AIBN (0.021g, 2 wt % relative to the total amount of monomer DMVP and cross-linker EGDMA), DMVP (0.5 mL, 3.25 mmol), and EGMDA (0.5 mL, 2.65 mmol) were then introduced into the solution. In a heating mantle, the mixture was heated to the boiling state from room temperature within 10 min. Then, the precipitation−polymerization was allowed to proceed under reflux conditions with solvent distilled off for 80 min. The resultant poly(DMVP-*co*-EGDMA) functionalized MWCNTs were collected by centrifugation and washed with water two times and ethanol two times via repeated resuspension, centrifugation, and decantation. Finally, the product was obtained by drying under vacuum at 80 °C for 24 h.

MWCNT/poly(MAA-*co*-EGDMA)s and MWCNT/poly(St-*co*-DVB)s were synthesized by a similar method, and the synthetic procedures are briefly introduced below. For the synthesis of MWCNT/poly(MAA-*co*-EGDMA)s, 0.04 g of MPS-CNTs was dispersed in 80 mL of acetonitrile. Then, AIBN (0.012 g), MAA (0.3 mL, 3.51 mmol), and EGDMA (0.3 mL, 1.59 mmol) were added into the above mixture. The mixture was heated to boiling state and kept under reflux conditions with solvent distilled off for 80 min. The resultant product was collected by centrifugation and washed with water two times and ethanol two times followed by drying treatment.

For the synthesis of MWCNT/poly(St-*co*-DVB)s, 0.04 g of MPS-CNTs was dispersed in 80 mL of acetonitrile. Then, AIBN (0.022 g), St (0.6 mL, 6.36 mmol), and DVB (0.6 mL, 5.02 mmol) were added into the above mixture. The mixture was heated to boiling state and kept under reflux conditions with solvent distilled off for 80 min. The resultant product was collected by centrifugation and washed with toluene two times and ethanol two times followed by drying treatment.

The MWCNT/poly(DMVP-*co*-EGDMA)s were transformed into MWCNT/poly(vinylphosphonic acid-*co*-EGDMA)s (poly(VPA-*co*-EGDMA)s) by hydrolyzing DMVP in aqueous hydrochloric acid.[31] MWCNT/poly(DMVP-*co*-EGDMA) powders (0.5 g) were mixed with excessive hydrochloric acid (30 mL, 10 mol L^{-1}) and stirred at 100 °C for 24 h. The powders were gathered by centrifugation and washed with water two times and ethanol two times via repeated resuspension, centrifugation, and decantation. Finally, the product was obtained by drying under vacuum at 80 °C for 24 h. MWCNT/poly(St-*co*-DVB)s were sulfonated by concentrated H_2SO_4 and trifluoromethanesulfonic anhydride (Tf_2O) in nitromethane.[32] A mixture of concentrated H_2SO_4 (0.151 mL), Tf_2O (0.434 mL), MWCNT/poly(St-*co*-DVB)s (0.3 g), and nitromethane (20 mL) was stirred at 30 °C for 4 h. The resultant product was collected by centrifugation and washed with toluene two times and ethanol two times followed by drying treatment. MWCNT/poly(VPA-*co*-EGDMA)s, MWCNT/poly(MAA-*co*-EGDMA)s, and sulfonated MWCNT/poly(St-*co*-DVB)s were designated as PCNTs, CCNTs, and SCNTs, respectively.

Poly(VPA-*co*-EGDMA) nanoparticles were synthesized by the same protocol as PCNTs (same AIBN/monomer/cross-linker/acetonitrile weight ratio) except for using MPS modified silica spheres as templates followed by etching silica via HF solution (10 wt %). The specific synthetic procedure was reported in the reference.[31] Poly(MAA-*co*-EGDMA) and sulfonated poly(St-*co*-DVB) nanoparticles were synthesized by the same protocol as CCNTs and SCNTs, respectively, but without using any templates. These polymer nanoparticles were obtained through the treatment of centrifugation, washing, and drying, and used for analyzing the polymer content in FCNT by TGA.

2.3. Membrane Preparation. The solvent in the purchased Nafion solution was removed by drying at 60 °C. The obtained Nafion resin (0.35 g) was dissolved in DMA to obtain a homogeneous Nafion/DMA solution. A quantified amount of FCNTs was dispersed in DMA under ultrasonication. The FCNTs/DMA solution was then added into the Nafion/DMA solution with the aid of agitation for 2 h and ultrasonic irradiation for 1 h. Nafion occupied an amount of 5 wt % in the solution. The resultant solution was filtered and then cast onto a glass plate, followed by heating at 80 °C in an oven for 12 h, and then at 120 °C for another 10 h. The membrane was peeled off from the glass plate in water. All membranes were pretreated by a standard procedure: soaking in 3% H_2O_2 aqueous solution at 80 °C for 1 h, rinsing in water at 80 °C for 1 h, soaking in 1 M H_2SO_4 at 80 °C for 1 h, and finally rinsing again in water until neutral pH. The amount of FCNTs in the cast solution was varied to obtain composite membranes with different filler contents. The composite membranes were named Nafion/FCNT-X%, where FCNT includes PCNTs, CCNTs, or SCNTs, and X% (= 0.2, 1, 2.5, 5, and 10 wt %) stands for the filler content in Nafion. The Nafion control membrane was also fabricated for comparison and designated as recast Nafion. The thicknesses of all the membranes were 70−90 μm.

2.4. Characterizations. Electron micrographs of the FCNTs and the three types of polymer nanoparticles were obtained with a transmission electron microscopy (TEM, Tecnai G2 20 S-TWIN).

A field emission scanning electron microscope (SEM, Nanosem 430) was utilized to image the morphology of the membrane cross-section with a pretreatment of liquid nitrogen freeze-fracture and then gold spraying.

Functional groups in FCNT samples were determined by FTIR spectra using a Bruker Vertex 70 FTIR spectrometer with a resolution of 4 cm^{-1}. Zeta PALS (Brookhaven Instrument Cooperation) was utilized to record the zeta potential of the FCNTs and MPS-CNTs in water at room temperature.

TGA was performed on a thermogravimetric analyzer (NETZSCH, TG209 F3) heating from 30 to 780 °C under nitrogen atmosphere at a rate of 10 °C min^{-1}. To obtain the polymer content (poly(VPA-*co*-EGDMA)) in PCNTs, TGA curves of poly(VPA-*co*-EGDMA) nanoparticles, MPS-CNTs, and PCNTs were measured. The ratios of weight loss (150−780 °C) to the weight at 150 °C (dry sample) were calculated for the three samples. The polymer content in PCNTs was obtained by analyzing the three ratios. The polymer contents in CCNTs and SCNTs were obtained by the same method as that used with PCNTs. The glass-transition temperatures (T_g) were detected utilizing a NETZSCH DSC (204, F1) instrument under nitrogen protection. Samples were treated by the following procedure: heating from 40 to 200 °C to remove any thermal history (10 °C/min), cooling to 60 °C (10 °C/min), and heating to 200 °C (10 °C/min).

2.5. Measurements. Water uptake and dimensional swelling of the membrane samples were measured by the following method. The sample was dried in a vacuum oven at 80 °C for 24 h. Its weight (W_{dry}), length (L_{dry}), and thickness (T_{dry}) were measured. After immersing it in water at a defined temperature (25 or 80 °C), its weight (W_{wet}), length (L_{wet}), and thickness (T_{wet}) were measured immediately. The procedure was performed three times to average the measured values. Water uptake and dimensional swelling were calculated by the following equations:

$$\text{water uptake (\%)} = \frac{W_{wet} - W_{dry}}{W_{dry}} \times 100 \quad (1)$$

$$\Delta T\ (\%) = \frac{T_{wet} - T_{dry}}{T_{dry}} \times 100 \quad (2)$$

$$\Delta L\ (\%) = \frac{L_{wet} - L_{dry}}{L_{dry}} \times 100 \quad (3)$$

Mechanical property measurement of the dry membranes was performed on an electronic tensile machine (WDW-2, Yangzhou Zhongke Measuring Apparatus Co., China) at a stretching rate of 20 mm min^{-1} at room temperature. The sizes of the samples were approximately 10 × 30 mm. The thicknesses of the samples are shown in Table S2 (see the Supporting Information). Reported values in Table 2 are the average of three samples.

The resistance value (R) was tested by two-point probe alternating current (AC) impedance spectroscopy with a frequency range of 10^5−1 Hz using an electrode system connected with a frequency response

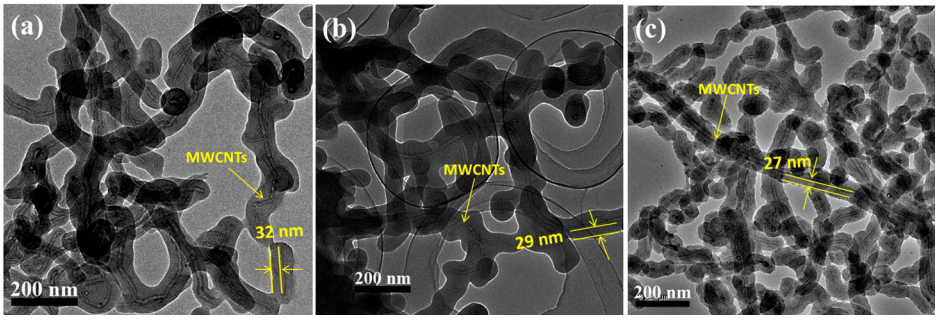

Figure 2. TEM images of FCNTs: (a) PCNTs, (b) CCNTs, and (c) SCNTs.

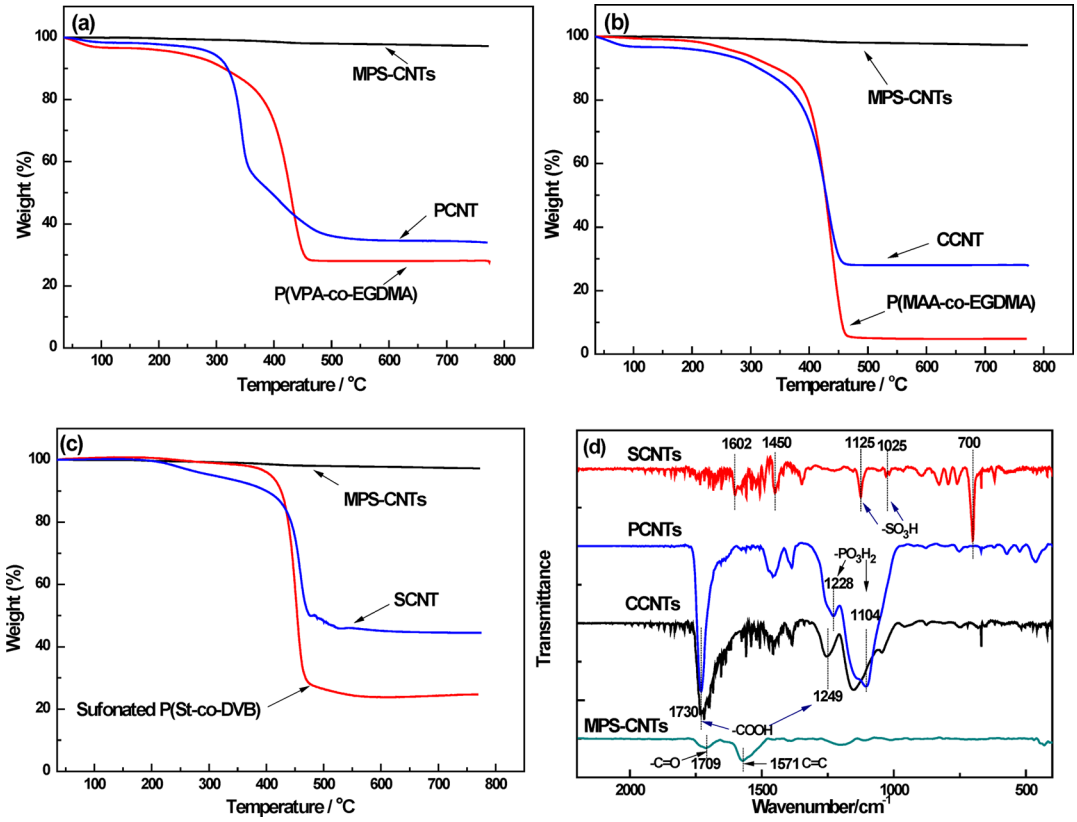

Figure 3. (a, b, and c) TGA curves of MPS-CNTs, FCNT, and the functionalized polymer in FCNT; (d) FTIR of the MPS-CNTs and FCNTs.

analyzer (FRA, Compactstat, IVIUM Tech.). Proton conductivity under 100% RH was measured in a temperature-controlled water-bath chamber where a sample was pressed by two parallel platinum electrodes. Proton conductivity under low RH at 80 °C was tested in a temperature-controlled sealed chamber in which the humidity was controlled by saturated salt solution held by a small container.[22] The saturated salt solutions used to control humiditiy are as follows: LiCl (10. 5%), K_2CO_3 (41.1%), and $NaNO_3$ (65.4%). Proton conductivity (σ, S cm^{-1}) was calculated using eq 4:

$$\sigma = \frac{l}{AR} \tag{4}$$

in which R is the membrane resistance, A is the cross-section area of the sample, and l is the length between the electrodes. Each sample was tested three times, and the average value of proton conductivity was calculated.

3. RESULTS AND DISCUSSION

3.1. Synthesis of Functionalized MWCNTs. Figure 1 illustrated the synthetic approach to functionalizing MWCNTs via surface-initiated distillation−precipitation−polymerization and the proposed structure of FCNTs.[16,33] Hydrolyzation and sulfonation were performed to render $-PO_3H_2$ groups for PCNTs and $-SO_3H$ groups for SCNTs, respectively. Distillation−precipitation−polymerization was selected as the synthetic technique because it is a straightforward and highly efficient protocol to generate a uniform polymeric cross-linked shell on the surface with carbon−carbon double bonds.[16] Distillation−precipitation−polymerization has been successfully employed for the synthesis of silica/polymer double-walled hybrid nanotubes[34] and the ellipsoidal hematite/polymer/titania multilayer hybrid materials.[35] Herein, hydroxylated MWCNTs were first modified with MPS to introduce vinyl groups, followed by *in situ* growth of polymer chains. During the polymerization, the MPS-CNTs captured the newly formed oligomers and monomers via the vinyl groups.

The TEM images of FCNTs in Figure 2 revealed that the three types of polymer network were uniformly covered over the MWCNTs. The average thicknesses of polymer layers in

PCNTs, CCNTs, and SCNTs were 32, 29, and 27 nm, respectively. The thickness was controlled through varying the (monomer + cross-linker)/MPS-CNTs feed ratio and polymerization time. By altering the (MAA + EGDMA)/MPS-CNTs feed ratio and polymerization time, the thickness of the polymeric layer in CCNTs changed from 11 to 35 nm (see Table S1 and Figure S3 in the Supporting Information). The corresponding polymer nanoparticles (poly(VPA-*co*-EGDMA), poly(MAA-*co*-EGDMA), and sulfonated poly(St-*co*-DVB) nanoparticles) were synthesized by the same protocol as FCNTs, and their TEM images are shown in the Supporting Information. FTIR spectra in Figure 3 indicate the functional groups in the MPS-CNTs and functionalized MWCNTs. In the MPS-CNTs sample, the peaks at 1571 and 1709 cm^{-1} corresponded to the stretching vibrations of the vinyl groups and carbonyl groups of the grafted MPS, respectively, demonstrating the successful modification of MPS on the MWCNTs. For the PCNTs sample, the characteristic peaks of $-PO_3H_2$ groups were shown at 1228 and 1104 cm^{-1} (corresponding to P═O and P−O stretching vibration, respectively), and the peak at 1730 cm^{-1} was caused by the C═O stretching vibration in polyEGDMA segments. For the CCNTs sample, the peaks at 1730 and 1249 cm^{-1} were due to the C═O and C−O stretching vibration from the poly(MAA-EGDMA) segments, verifying the presence of −COOH groups. For the SCNTs sample, $-SO_3H$ displayed typical adsorption peaks at 1125 and 1025 cm^{-1}, and the peaks at 1602, 1450, and 700 cm^{-1} were caused by the benzyl ring. These successful functionalizations were further confirmed by their electronegativity change after polymerization, which was revealed by the zeta-potentials as listed in Table 1. The zeta-potential of MPS-CNTs was −4.01 mV.

Table 1. Thickness of the Grafted Polymer Layer, Polymer Content, and Zeta Potential of the FCNTs

FCNTs	thickness of polymer layer (nm)	polymer content[a] (wt %)	zeta potential (mV)
PCNTs	32 ± 5	93.3	−10.38
CCNTs	29 ± 6	74.1	−12.15
SCNTs	27 ± 3	72.7	−11.57

[a]Polymer content was obtained though an analysis of the TGA curves in Figure 3.

Figure 3 showed the TGA curves of MPS-modified MWCNT, FCNT, and the functionalized polymer in FCNT. The ratios of functionalized polymer in FCNTs were obtained based on the TGA results and displayed in Table 1. The grafted polymer chains in PCNT, CCNT, and SCNT reached the ratios of 93.3, 74.1, and 72.7 wt %, respectively, after 80 min of polymerization. These graft yields were remarkably high when compared with the previously reported results. For example, 77.9 wt % of polystyrene was grafted on MWCNTs via *in situ* ATRP at 100 °C for 50 h.[36] The high graft yields may have originated for the following reasons: (i) because acetonitrile was a poor solvent for the newly formed oligomers, the oligomers could precipitate out of the solvent.[16] The reactive sites were condensed after the precipitation of the oligomers on the MWCNTs during the polymerization. (ii) The distillation of solvent out of the reaction system could increase the concentrations of the reactants. All samples exhibited two-stage weight loss. The first weight loss region (30−150 °C) was attributed to the evaporation of water, and the second weight loss region (150−780 °C) was ascribed to the decomposition of functional groups and polymer chains. The residual mass of the polymer decreased in the order: P(VPA-*co*-EGDMA) (34.4%) > sulfonated P(St-*co*-DVB) (24.7%) > P(MAA-*co*-EGDMA) (4.9%), in agreement with the reported results.[18,37]

Electrical conductivity of CNTs endowed the composite membranes with the risk of short circuit, which can be circumvented by maintaining the contents of CNTs below the percolation threshold (2 wt %).[38] Because the polymer contents in FCNTs were greater than 72.7 wt %, short circuit can be avoided by keeping the content of FCNTs below 7.3 wt %. Moreover, the MWCNTs were completely covered by the thick polymer layer, which can impede electron conduction. Thus, it can be conjectured that a short circuit could not occur in the composite membrane.

3.2. Morphologies and Thermal Properties of the Membranes. SEM images in Figure 4 displayed the cross-sectional morphologies of the membranes. Filler dispersion is a key factor determining various properties of the composite membrane such as mechanical stability and proton conductivity.[23,39] The observed excellent dispersion of polymer functionalized MWCNTs within Nafion can be attributed to their efficient thermodynamic wetting with the polymer matrix.[39] In comparison with other samples, the morphologies of Nafion/PCNTs samples were more significantly influenced by the incorporation of PCNTs, possibly because the electrostatic repulsion between Nafion chains and PCNTs were stronger than that between Nafion chains and CCNTs or SCNTs. The Nafion/CCNTs-10% sample showed more obvious aggregation of CCNTs, which may be originated from the easier formation of hydrogen bonding between −COOH groups compared with that between $-PO_3H_2$ or between $-SO_3H$ groups.

The TGA of the membranes (Figure 5) under N_2 atmosphere indicated that the incorporation of FCNTs enhanced the thermal stabilities of Nafion based composite membranes. The onset decomposition temperature enhanced from 301.3 °C of recast Nafion to 311.4 °C of Nafion/SCNT-5%, 327.3 °C of Nafion/CCNT-5%, and 327.8 °C of Nafion/PCNT-5%. In comparison, Nafion/SCNT-5% showed a lower onset decomposition temperature because $-SO_3H$ groups have a lower thermal stability. All samples showed three typical stages of weight loss. The weight losses at 30−200 °C, 250−380 °C, and 380−780 °C were ascribed to membrane dehydration, loss of functional groups, and decomposition of polymer main chains, respectively. The ratios of sample decomposition at 200−780 °C to the corresponding dehydrated sample were 95.3% for recast Nafion, 86.8% for Nafion/PCNT-5%, 87.9% for Nafion/CCNT-5%, and 88.9% for Nafion/SCNT-5%. Compared with recast Nafion, the composite membranes showed lower decomposition ratios, which were mainly caused by the superior thermal stability of MWCNTs.

The DSC curves in Figure 6 indicated the glass transition temperature (T_g) of the membranes. The T_g of recast Nafion was 125.6 °C in good agreement with the literature value.[40] In comparison, the composite membranes displayed lower T_g, suggesting the increased mobility of Nafion chains. The decreasing order of T_g was Nafion/SCNT-5% (118.5 °C), Nafion/CCNT-5% (117.8 °C), and Nafion/PCNT-5% (112.2 °C). This result revealed that the interface interactions between the Nafion matrix and PCNTs were weaker than that of Nafion matrix/CCNTs and Nafion matrix/SCNTs. Because both

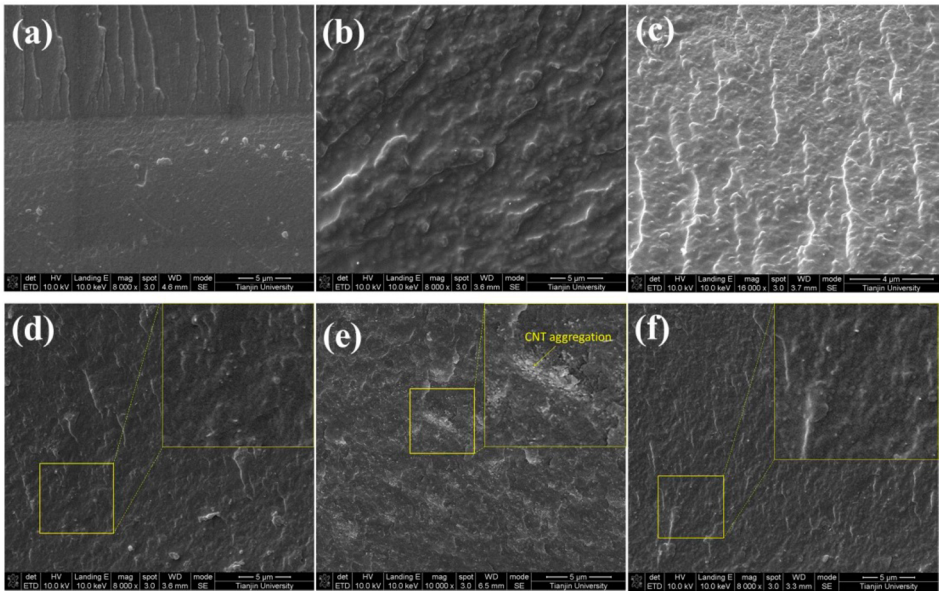

Figure 4. SEM micrographs of cross-sections: (a) recast Nafion, (b) Nafion/PCNT-5%, (c) Nafion/PCNT-10%, (d) Nafion/CCNT-5%, (e) Nafion/CCNT-10%, and (f) Nafion/SCNT-5%.

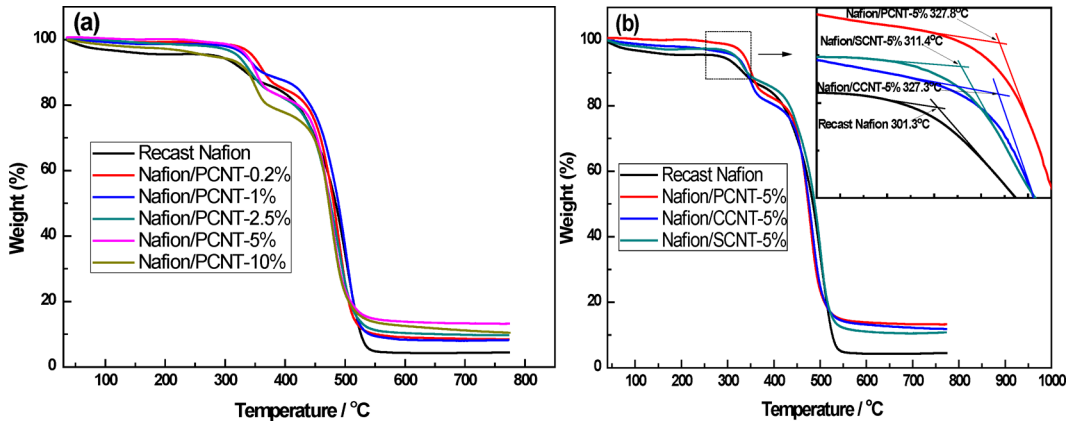

Figure 5. TGA curves of the membranes: (a) PCNTs incorporated composite membranes and the recast Nafion membrane and (b) 5 wt % FCNTs incorporated composite membranes and the recast Nafion membrane with the inset indicating onset decomposition temperature.

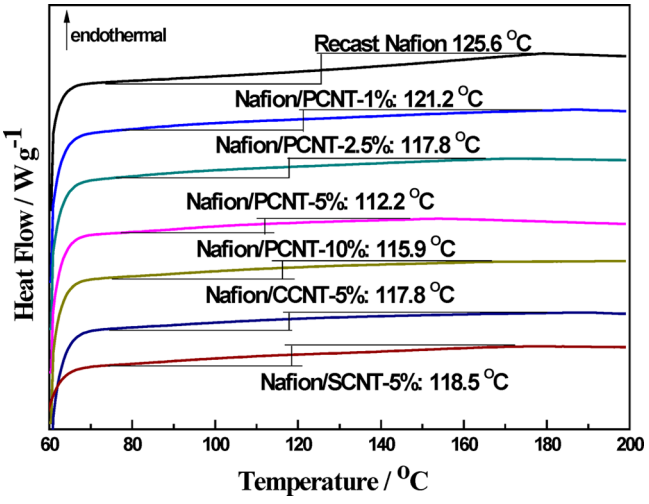

Figure 6. DSC curves of the membranes.

FCNTs and Nafion chains are electronegative, the weakened interface interactions may be caused by the increased electrostatic repulsion within the Nafion/FCNTs interface. When the PCNT content was below 5 wt %, the T_g of Nafion/PCNT decreased with increased filler content, reflecting that the mobility of more Nafion chains was increased with increasing filler content. When the filler content was further increased to 10 wt %, the T_g increased to 115.9 °C, which may be due to the fact that the aggregation of PCNTs reduced the Nafion/PCNTs interfaces, thus weakening the influence of PCNTs on the chain mobility of Nafion.

3.3. Water Uptake and Dimensional Change of the Membranes. Water uptake is an important parameter because water is the medium to transport protons, and higher water uptake can engender higher proton conductivity.[22] Table 2 showed that the incorporation of FCNTs enhanced the water uptake of the composite membranes, and the water uptake increased with FCNTs contents. For example, the water uptake increased from 28.8 wt % (25 °C) and 46.8 wt % (80 °C) for recast Nafion to 37.6 wt % (25 °C, 30.6% increment) and 59.6 wt % (80 °C, 27.4% increment), respectively, for Nafion/PCNT-10%. The enhancements of water uptake were possibly due to the following reasons with decreasing importance. (i)

Table 2. Dimensional Swelling, Water Uptake, Proton Conductivity, and Mechanical Properties of the Membranes

	dimensional swelling (%)[a]				water uptake		conductivity (80 °C)		mechanical properties[a]		
	ΔT(thickness)		ΔL(in plane)		(wt %)[a]		(mS cm^{-1})[a]		tensile strength	Young's modulus	elongation at break
membranes	25 °C	80 °C	25 °C	80 °C	25 °C	80 °C	100% RH	41.1% RH	(MPa)	(GPa)	(%)
recast Nafion	18.4	27.3	13.2	19.6	28.8	46.8	137	4.54	18.4	0.085	320
Nafion/PCNT-0.2%	20.3	27.7	12.8	18.8	29.6	48.9	147	4.89	29.1	0.157	304
Nafion/PCNT-1%	20.6	28.1	11.5	17.1	32.1	52.8	179	6.04	29.7	0.111	338
Nafion/PCNT-2.5%	22.9	29.6	11.1	16.7	33.2	54.6	197	8.59	25.8	0.137	228
Nafion/PCNT-5%	23.2	30.8	10.7	15.9	35.4	56.6	198	15.01	18.1	0.132	132
Nafion/PCNT-10%	21.8	27.4	10.3	15.1	37.6	59.6	165	6.70	21.8	0.178	170
Nafion/CCNT-1%	19.7	28.4	12.3	18.0	29.7	47.7	168	5.22	24.4	0.119	274
Nafion/CCNT-2.5%	21.4	29.9	11.1	17.0	31.5	49.7	184	6.09	18.8	0.134	199
Nafion/CCNT-5%	22.0	30.4	10.3	16.5	32.3	52.1	156	10.37	14.8	0.142	153
Nafion/CCNT-10%	18.6	28.3	11.9	16.8	36.9	55.7	141	6.17	14.9	0.212	47
Nafion/SCNT-1%	18.7	29.9	11.9	18.7	29.2	47.3	174	4.93	22.4	0.134	290
Nafion/SCNT-2.5%	19.5	28.3	10.3	16.2	31.3	49.5	192	5.80	17.5	0.141	209
Nafion/SCNT-5%	20.1	30.9	9.5	14.6	33.2	51.2	193	7.15	15.1	0.143	103
Nafion 117	10.9	17.4	9.4	15.9	18.1	25.2	168	7.58	22.3	0.122	345

[a]Average values for dimensional swelling, water uptake, conductivity, and mechanical properties are shown with a standard error of 6%, 8%, 5%, and 10%, respectively.

The hydrophilic shells of FCNTs can interact with water via hydrogen or electrostatic bonds; (ii) the cavity of FCNTs can store water; and (iii) the incorporation of fillers into the Nafion matrix could lead to void spaces between the Nafion matrix and the fillers. This possibility was supported by the fact that elongation at break decreased significantly with increasing filler content (see the following discussion related to mechanical properties) and that (iv) the flexibility of Nafion chains at the hybrid interfaces was augmented (demonstrated by DSC results) rendering more room for water.

Dimensional stability (listed in Table 2) revealed that the incorporation of FCNTs restrained the in-plane swelling and fomented the through-plane swelling. For Nafion/PCNT-5%, the in-plane swelling reduced by 18.9% at 25 °C, and the through-plane swelling increased by 26.1% at 25 °C compared with those of recast Nafion. The enhanced through-plane swelling was possibly due to the swollen hydrophilic shells of FCNTs and increased mobility of Nafion chains at the hybrid interfaces. The enhanced anisotropic swelling behavior (larger dimensional change in the through-plane direction than that in the in-plane direction) may have originated from the fact that FCNTs tended to orient in the in-plane direction and performed the role of restricting in-plane swelling. This enhanced anisotropic swelling behavior is favorable for preparing membrane electrode assembly because it is important to restrict the in-plane swelling in order to inhibit delamination of the catalyst layer.[41]

3.4. Mechanical Properties. Typical stress−strain curves for recast Nafion and composite membranes are shown in Figure 7, and the mechanical properties are summarized in Table 2. The incorporation of FCNTs significantly reinforced Nafion membranes. For the composite membrane loaded with 1 wt % filler, their tensile stress and Young's modulus were remarkably higher than those of recast Nafion. For Nafion/PCNT-1%, the tensile strength and Young's modulus increased by 61.4% and 30.6%, respectively, in comparison with recast Nafion. The reinforced effect was due to the effective transfer of the mechanical load to FCNTs in the composite, which was promoted by the good interface compatibility between FCNTs and Nafion matrix.[11] With increased filler contents (precluding Nafion/PCNT-0.2% and -10%), the composite membrane

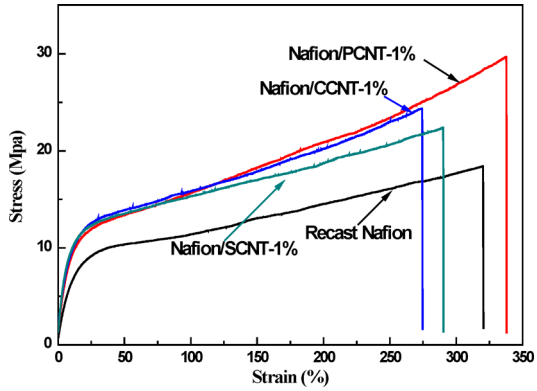

Figure 7. Stress−strain curves for some typical membranes at room temperature.

showed a higher Young's modulus and lower tensile stress and elongation at break. Nafion/CCNT-10% displayed the highest Young's modulus of 0.212 GPa, 1.5 times higher than that of recast Nafion. The considerable decrease of elongation at break with increasing filler content may be due to the fact that as the loading of FCNTs increased there was more void space in the membrane, which, in turn, caused breakage at a smaller elongation value. Nafion/CCNT-10% showed remarkably low elongation at break, possibly caused by the fact that the aggregation of CCNTs as observed by SEM generated a large amount of void space. These behaviors were common for CNT-incorporated composites.[11,42,43] These results indicated that the FCNTs were effective in reinforcing Nafion and that the composite membranes were sufficiently tough and ductile for potential PEM application.

3.5. Proton Conductivity. Proton conductivities of the membranes under 100% RH at 80 °C are listed in Table 2. The proton conductivity of recast Nafion was 0.137 S cm^{-1}, in agreement with the reported result.[44] In comparison, all composite membranes showed enhanced proton conductivity. For instance, the proton conductivities increased to 0.198 S cm^{-1} for Nafion/PCNTs-5% (44.5% increment), to 0.184 S cm^{-1} for Nafion/CCNT-2.5% (34.3% increment), and to 0.193 S cm^{-1} for Nafion/SCNT-2.5% (40.9% increment). These

dx.doi.org/10.1021/am503760u | ACS Appl. Mater. Interfaces 2014, 6, 15291−15301

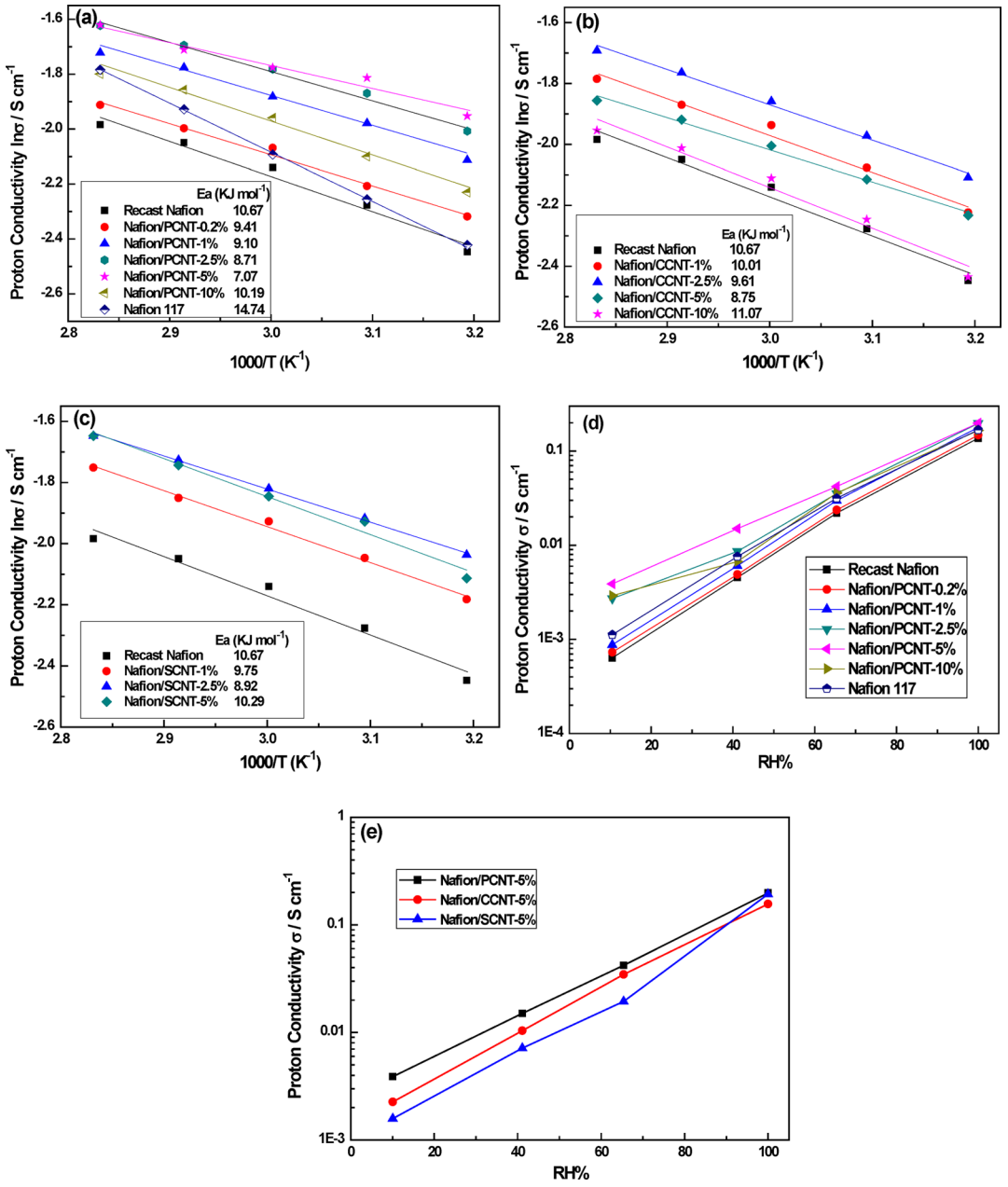

Figure 8. Temperature-dependent proton conductivities of the composite membranes with recast Nafion and Nafion 117 as comparison: (a) Nafion/PCNTs, (b) Nafion/CCNTs, and (c) Nafion/SCNTs. Humidity-dependent proton conductivities of the membrane: (d) Nafion/PCNTs with recast Nafion and Nafion 117 as comparison, and (e) 5 wt % filler incorporated composite membranes.

enhancements were attributed to the following two reasons: (i) the proton-conduction polymers grafted on the MWCNTs may construct continuous pathways for rapid proton transport. Moreover, the $-SO_3H$ on Nafion chains assembled with the FCNTs via hydrophilc interactions in the interfacial region could further enhance the efficacy of proton transport along the continuous pathways; (ii) the incorporation of FCNTs enhanced the mobility of Nafion chains at the hybrid interfaces (demonstrated by DSC results), benefiting proton transport. When the filler contents were below 2.5 wt %, the proton conductivities augmented remarkably with increasing filler contents. However, further increasing filler contents slightly enhanced or deteriorated the proton conductivites, possibly on account of the aggregation of FCNTs (see SEM characterization in Figure 4), which weakened their roles as continuous pathways for facile proton transport and damaged the phase-separated morphology of Nafion. Comparing the proton conductivities of Nafion/PCNTs, Nafion/CCNTs, and Nafion/SCNTs, it can be found that the proton conductivities under the identical filler content decreased in the order of Nafion/PCNTs > Nafion/SCNTs > Nafion/CCNT. This behavior was not in agreement with the fact that the proton-conduction capacity of functional groups decreased in the order of $-SO_3H$ > $-PO_3H_2$ > $-COOH$ under 100% RH.[45] The reason was that the SCNTs were cross-linked by DVB, which was more rigid than EGDMA (cross-linker for PCNTs and CCNTs) leading to reduced mobility and water uptake of polymer chains in SCNTs.[18]

To further elucidate the proton transport properties, Arrhenius activation energy (*Ea*) was calculated from the

temperature-dependent proton conductivities under 100% RH at 80 °C, as shown in Figure 8. All composite membranes except Nafion/CCNT-10% revealed lower *Ea* than that for recast Nafion, indicating that less energy was needed for proton transport and that lower-energy-barrier pathways were constructed.[46] The enhanced *Ea* for Nafion/CCNT-10% was ascribed to the fact that the continuity of proton transport pathways was obstructed by the aggregation of CCNTs, as observed from the SEM image. For Nafion/PCNTs, the *Ea* decreased from 9.41 to 7.07 kJ mol^{-1} with PCNT content increasing from 0.2 wt % to 5 wt %, indicating that more lower-energy-barrier pathways were created. However, the *Ea* increased to 10.19 kJ when the filler content increased to 10 wt %, which was also ascribed to the obstruction of proton transport pathways caused by filler aggregation. The *Ea* variation tendency was considerably in accordance with the variation tendency of proton conductivities under 100% RH at 80 °C, indicating the fact that the increase of proton conductivities with increased filler contents was due to the construction of continuous proton transport pathways (lower-energy-barrier), and the decrease of proton conductivities with increased filler contents was due to the obstruction of continuous proton transport pathways caused by filler aggregation.

Proton conductivities under reduced RH at 80 °C are summarized in Table 2 and Figure 8. All composite membranes displayed higher proton conductivities than that of the recast Nafion. Table 2 shows that proton conductivities under 41.1% RH at 80 °C increased from 4.54 mS cm^{-1} for the recast Nafion to 15.01 mS cm^{-1}, 10.37 mS cm^{-1}, and 7.15 mS cm^{-1} for Nafion/PCNT-5% (230.6% increment), Nafion/CCNT-5% (128.4% increment), and Nafion/SCNT-5% (57.5% increment), respectively. The efficacy of promoting proton conductivities of Nafion under 41.1% RH decreased in the order of PCNTs > CCNT > SCNT. These phenomena can be explained as follows. Compared with $-SO_3H$ and $-COOH$ groups, $-PO_3H_2$ groups perform the best in transporting protons under low RH because $-PO_3H_2$ groups are more ready to form percolated hydrogen-bonding networks under low RH.[47] Moreover, water plays a vital role in transporting protons, and proton conductivity of the membrane under low RH is highly dependent on its water retention properties.[27] The cross-linked hydrophilic shells of FCNTs can retain water via hydrophilic interactions and capillary force, rendering FCNTs with excellent water retention properties.[29,30] The proton conduction capacity of $-SO_3H$ groups is significantly higher than that of $-COOH$ groups, interpretating why Nafion/SCNT was more conductive than Nafion/CCNT under 100% RH. However, Nafion/SCNT showed a lower conductivity than that of Nafion/CCNT under 41.1% RH. This is because the structure of SCNTs cross-linked by DVB was more hydrophobic, leading to lower water retention properties.[18]

The humidity dependence of proton conductivity at 80 °C (Figure 8) revealed that Nafion/PCNT-5% possessed the least reliance of proton conductivity on humidity. Compared with recast Nafion, Nafion/PCNT-5% showed increased proton conductivities by 43.7% at 100% RH, by 92.0% at 65.4% RH, by 230.6% at 41.1% RH, and by 510.6% at 10.5% RH. The enhancement of proton conductivity increased with decreased RH. This behavior can be attributed to the water-retention properties afforded by the hydrophilic cross-linked shells of PCNTs and the high proton-conduction capacity of $-PO_3H_2$ groups under low RH.[29,47] Various hydrophilic fillers have been employed to increase the proton conductivity under low RH.[48,49] Incorporation of superacidic electrospun fiber into Nafion rendered the composite membrane a proton conductivity 455.6% times higher than that of recast Nafion under 20% RH at 80 °C, which was owing to the construction of a network of continuous proton pathways.[49] This study validated the incorporation of the FCNTs (especially PCNTs) in elevating the proton conductivity of Nafion under reduced RH.

4. CONCLUSIONS

An approach to functionalizing MWCNTs with cross-linked polymer via surface-initiated distillation−precipitation−polymerization was reported for the first time. Three types of cross-linked polymers (poly(VPA-*co*-EGDMA), poly(MAA-*co*-EGDMA), and sulfonated poly(St-*co*-DVB)) were *in situ* grafted on MWCNTs. The grafted polymer layers with thickness around 30 nm were uniformly covered on the MWCNTs, and the thickness was finely controlled through varying (monomer + cross-linker)/MPS-CNTs feed ratio and polymerization time. The graft yield reached up to 93.3 wt % after 80 min of polymerization. The resultant FCNTs were homogeneously incorporated into the Nafion matrix to prepare composite membranes. The composite membranes exhibited significantly enhanced proton conductivities under reduced RH in comparison with those of recast Nafion. Nafion/PCNT-5% showed the least dependence on humidity, and its proton conductivities increased by 43.7% at 100% RH, by 92.0% at 65.4% RH, by 230.6% at 41.1% RH, and by 510.6% at 10.5% RH. The conductivity enhancement was primarily attributed to the construction of continuous proton transport pathways (lower-energy-barrier) within membranes enabled by PCNTs, excellent water-retention properties of the cross-linked polymer in PCNTs, and high proton conductivity of $-PO_3H_2$ groups. Moreover, the incorporation of FCNTs increased the mechanical performance of Nafion membranes. The tensile strength and Young's modulus of Nafion/PCNT-1% increased by 61.4% and 30.6%, respectively, due to the good interface compatibility between FCNTs and Nafion matrix. The distillation−precipitation−polymerization approach can be extended to functionalize a variety of carbon nanomaterials and prepare a variety of composite membranes.

■ ASSOCIATED CONTENT

Ⓢ Supporting Information

TEM of the functionalized polymer nanoparticles, MPS-CNTs, and CCNTs synthesized by different formulas, SEM of MPS-CNTs, thickness of the samples for the measurement of mechanical properties, and relevant discussions. This material is available free of charge via the Internet at http://pubs.acs.org.

■ AUTHOR INFORMATION

Corresponding Author

*Tel: 86-22-27406646. Fax: 86-22-23500086. E-mail: zhyjiang@tju.edu.cn.

Notes

The authors declare no competing financial interest.

■ ACKNOWLEDGMENTS

We thank the National Science Fund for Distinguished Young Scholars (21125627) and the Program of Introducing Talents of Discipline to Universities (B06006) for financial support.

REFERENCES

(1) Karousis, N.; Tagmatarchis, N. Current Progress on the Chemical Modification of Carbon Nanotubes. *Chem. Rev.* **2010**, *110*, 5366−5397.

(2) Wang, Q. H.; Bellisario, D. O.; Drahushuk, L. W.; Jain, R. M.; Kruss, S.; Landry, M. P.; Mahajan, S. G.; Shimizu, S. F. E.; Ulissi, Z. W.; Stran, M. S. Low Dimensional Carbon Materials for Applications in Mass and Energy Transport. *Chem. Mater.* **2014**, *26*, 172−183.

(3) Schnorr, J. M.; Swager, T. M. Emerging Applications of Carbon Nanotubes. *Chem. Mater.* **2011**, *23*, 646−657.

(4) Sakellariou, G.; Priftis, D.; Baskaran, D. Surface-Initiated Polymerization from Carbon Nanotubes: Strategies and Perspectives. *Chem. Soc. Rev.* **2013**, *42*, 677−704.

(5) Gorityala, B. K.; Ma, J.; Wang, X.; Chen, P.; Liu, X. W. Carbohydrate Functionalized Carbon Nanotubes and their Applications. *Chem. Soc. Rev.* **2010**, *39*, 2925−2934.

(6) Chen, W. F.; Wu, J. S.; Kuo, P. L. Poly(oxyalkylene)diamine-Functionalized Carbon Nanotube/Perfluorosulfonated Polymer Composites: Synthesis, Water State, and Conductivity. *Chem. Mater.* **2008**, *20*, 5756−5767.

(7) Khare, K. S.; Khabaz, F.; Khare, R. Effect of Carbon Nanotube Functionalization on Mechanical and Thermal Properties of Cross-Linked Epoxy-Carbon Nanotube Nanocomposites: Role of Strengthening the Interfacial Interactions. *ACS Appl. Mater. Interfaces* **2014**, *6*, 6098−6110.

(8) Liao, W. H.; Tien, H. W.; Hsiao, S. T.; Li, S. M.; Wang, Y. S.; Huang, Y. L.; Yang, S. Y.; Ma, C. C. M.; Wut, Y. F. Effects of Multiwalled Carbon Nanotubes Functionalization on the Morphology and Mechanical and Thermal Properties of Carbon Fiber/Vinyl Ester Composites. *ACS Appl. Mater. Interfaces* **2013**, *5*, 3975−3982.

(9) Yuan, W.; Chan-Park, M. B. Covalent cum Noncovalent Functionalizations of Carbon Nanotubes for Effective Reinforcement of a Solution Cast Composite Film. *ACS Appl. Mater. Interfaces* **2012**, *4*, 2065−2073.

(10) Sahoo, N. G.; Rana, S.; Cho, J. W.; Li, L.; Chan, S. H. Polymer Nanocomposites Based on Functionalized Carbon Nanotubes. *Prog. Polym. Sci.* **2010**, *35*, 837−867.

(11) Spitalsky, Z.; Tasis, D.; Papagelis, K.; Galiotis, C. Carbon Nanotube−Polymer Composites: Chemistry, Processing, Mechanical and Electrical Properties. *Prog. Polym. Sci.* **2010**, *35*, 357−401.

(12) Moniruzzaman, M.; Winey, K. Polymer Nanocomposites Containing Carbon Nanotubes. *Macromolecules* **2006**, *39*, 5194−5205.

(13) Kong, H.; Gao, C.; Yan, D. Y. Controlled Functionalization of Multiwalled Carbon Nanotubes by in Situ Atom Transfer Radical Polymerization. *J. Am. Chem. Soc.* **2004**, *126*, 412−413.

(14) Hong, C. Y.; You, Y. Z.; Pan, C. Y. Synthesis of Water-Soluble Multiwalled Carbon Nanotubes with Grafted Temperature-Responsive Shells by Surface Raft Polymerization. *Chem. Mater.* **2005**, *17*, 2247−2254.

(15) Khan, M. U.; Gomes, V. G.; Altarawneh, I. S. Synthesizing Polystyrene/Carbon Nanotube Composites by Emulsion Polymerization with Non-Covalent and Covalent Functionalization. *Carbon* **2010**, *48*, 2925−2933.

(16) Li, G. L.; Mohwald, H.; Shchukin, D. G. Precipitation Polymerization for Fabrication of Complex Core-Shell Hybrid Particles and Hollow Structures. *Chem. Soc. Rev.* **2013**, *42*, 3628−3646.

(17) Li, L. Y.; Liu, G. Y.; Qin, D. B.; Yang, X. L. Synthesis of P(EGDMA-*co*-MAA)/P(EGDMA-*co*-VPy)/Titania/Polymer Tetra-Layer Microspheres. *Polym. Chem.* **2010**, *1*, 650−657.

(18) He, G.; Li, Y.; Li, Z.; Nie, L.; Wu, H.; Yang, X.; Zhao, Y.; Jiang, Z. Enhancing Water Retention and Low-Humidity Proton Conductivity of Sulfonated Poly(ether ether ketone) Composite Membrane Enabled by the Polymer-Microcapsules with Controllable Hydrophilicity−Hydrophobicity. *J. Power Sources* **2014**, *248*, 951−961.

(19) Zhang, H.; Shen, P. K. Advances in the High Performance Polymer Electrolyte Membranes for Fuel Cells. *Chem. Soc. Rev.* **2012**, *41*, 2382−2394.

(20) Zhang, H.; Shen, P. K. Recent Development of Polymer Electrolyte Membranes for Fuel Cells. *Chem. Rev.* **2012**, *112*, 2780−2832.

(21) Jiang, S. P. Functionalized Mesoporous Structured Inorganic Materials as High Temperature Proton Exchange Membranes for Fuel Cells. *J. Mater. Chem. A* **2014**, *2*, 7637−7655.

(22) Si, K.; Wycisk, R.; Dong, D.; Cooper, K.; Rodgers, M.; Brooker, P.; Slattery, D.; Litt, M. Rigid-Rod Poly(phenylenesulfonic acid) Proton Exchange Membranes with Cross-Linkable Biphenyl Groups for Fuel Cell Applications. *Macromolecules* **2013**, *46*, 422−433.

(23) Liu, Y.-L.; Su, Y.-H.; Chang, C.-M.; Suryani; Wang, D.-M.; J.-Y. Lai, D.-M. Preparation and Applications of Nafion-Functionalized Multiwalled Carbon Nanotubes for Proton Exchange Membrane Fuel Cells. *J. Mater. Chem.* **2010**, *20*, 4409.

(24) Kannan, R.; Kakade, B. A.; Pillai, V. K. Polymer Electrolyte Fuel Cells Using Nafion-Based Composite Membranes with Functionalized Carbon Nanotubes. *Angew. Chem., Int. Ed.* **2008**, *47*, 2653−2656.

(25) Chang, C.-M.; Li, H.-Y.; Lai, J.-Y.; Liu, Y.-L. Nanocomposite Membranes of Nafion and Fe_3O_4-Anchored and Nafion-Functionalized Multiwalled Carbon Nanotubes Exhibiting High Proton Conductivity and Low Methanol Permeability for Direct Methanol Fuel Cells. *RSC Adv.* **2013**, *3*, 12895.

(26) Kannan, R.; Parthasarathy, M.; Maraveedu, S. U.; Kurungot, S.; Pillai, V. K. Domain Size Manipulation of Perflouorinated Polymer Electrolytes by Sulfonic Acid-Functionalized MWCNTs to Enhance Fuel Cell Performance. *Langmuir* **2009**, *25*, 8299−8305.

(27) Li, N.; Guiver, M. D. Ion Transport by Nanochannels in Ion-Containing Aromatic Copolymers. *Macromolecules* **2014**, *47*, 2175−2198.

(28) Wang, J.; Yue, X.; Zhang, Z.; Yang, Z.; Li, Y.; Zhang, H.; Yang, X.; Wu, H.; Jiang, Z. Enhancement of Proton Conduction at Low Humidity by Incorporating Imidazole Microcapsules into Polymer Electrolyte Membranes. *Adv. Funct. Mater.* **2012**, *22*, 4539−4546.

(29) Wang, J.; Zhang, H.; Yang, X.; Jiang, S.; Lv, W.; Jiang, Z.; Qiao, S. Z. Enhanced Water Retention by Using Polymeric Microcapsules to Confer High Proton Conductivity on Membranes at Low Humidity. *Adv. Funct. Mater.* **2011**, *21*, 971−978.

(30) He, G.; Li, Z.; Li, Y.; Li, Z.; Wu, H.; Yang, X.; Jiang, Z. Zwitterionic Microcapsules as Water Reservoirs and Proton Carriers within a Nafion Membrane to Confer High Proton Conductivity under Low Humidity. *ACS Appl. Mater. Interfaces* **2014**, *6*, 5362−5366.

(31) Nie, L.; Dong, H.; Han, X.; He, G.; Wu, H.; Jiang, Z. Enhanced Proton Conductivity under Low Humidity of Sulfonated Poly(ether ether ketone) Composite Membrane Enabled by Multifunctional Phosphonic Acid Polymeric Submicrocapsules. *J. Power Sources* **2013**, *240*, 258−266.

(32) Li, Z.; He, G.; Zhao, Y.; Cao, Y.; Wu, H.; Li, Y.; Jiang, Z. Enhanced proton conductivity of proton exchange membranes by incorporating sulfonated metal-organic frameworks. *J. Power Sources* **2014**, *262*, 372−379.

(33) He, G.; Nie, L.; Han, X.; Dong, H.; Li, Y.; Wu, H.; He, X.; Hu, J.; Jiang, Z. Constructing Facile Proton-Conduction Pathway within Sulfonated Poly(ether ether ketone) Membrane by Incorporating Poly(phosphonic acid)/Silica Nanotubes. *J. Power Sources* **2014**, *259*, 203−212.

(34) Choi, B. Y.; Hong, J. H.; Park, Y. C.; Jung, D. H.; Hong, W. H.; Hammond, P. T.; Park, H. S. Innovative Polymer Nanocomposite Electrolytes: Nanoscale Manipulation of Ion Channels by Functionalized Graphenes. *ACS Nano* **2011**, *5*, 5167−5174.

(35) Li, L.; Qin, D.; Yang, X.; Liu, G. Synthesis of Ellipsoidal Hematite/Polymer/Titania Hybrid Materials and the Corresponding Hollow Ellipsoidal Particles. *Polym. Chem.* **2010**, *1*, 289.

(36) Kong, H.; Gao, C.; Yan, D. Y. Functionalization of Multiwalled Carbon Nanotubes by Atom Transfer Radical Polymerization and Defunctionalization of the Products. *Macromolecules* **2004**, *37*, 4022−4030.

(37) Aslan, A.; Bozkurt, A. Nanocomposite Polymer Electrolyte Membranes Based on Poly (vinylphosphonic acid)/Sulfated Nano-Titania. *J. Power Sources* **2012**, *217*, 158−163.

(38) Thomassin, J.-M.; Kollar, J.; Caldarella, G.; Germain, A.; Jérôme, R.; Detrembleur, C. Beneficial Effect of Carbon Nanotubes on the Performances of Nafion Membranes in Fuel Cell Applications. *J. Membr. Sci.* **2007**, *303*, 252−257.
(39) Li, Y.; He, G.; Wang, S.; Yu, S.; Pan, F.; Wu, H.; Jiang, Z. Recent Advances in the Fabrication of Advanced Composite Membranes. *J. Mater. Chem. A* **2013**, *1*, 10058.
(40) Jung, H.-Y.; Kim, J. W. Role of the Glass Transition Temperature of Nafion 117 Membrane in the Preparation of the Membrane Electrode Assembly in a Direct Methanol Fuel Cell (DMFC). *Int. J. Hydrogen Energy* **2012**, *37*, 12580−12585.
(41) Li, N.; Lee, S. Y.; Liu, Y.-L.; Lee, Y. M.; Guiver, M. D. A New Class of Highly-Conducting Polymer Electrolyte Membranes: Aromatic ABA Triblock Copolymers. *Energy Environ. Sci.* **2012**, *5*, 5346.
(42) Suryani; Chang, C.-M.; Liu, Y.-L.; Lee, Y. M. Polybenzimidazole Membranes Modified with Polyelectrolyte-Functionalized Multiwalled Carbon Nanotubes for Proton Exchange Membrane Fuel Cells. *J. Mater. Chem.* **2011**, *21*, 7480.
(43) Coleman, J. N.; Khan, U.; Blau, W. J.; Gun'ko, Y. K. Small but Strong: A Review of the Mechanical Properties of Carbon Nanotube−Polymer Composites. *Carbon* **2006**, *44*, 1624−1652.
(44) Wang, C.; Li, N.; Shin, D. W.; Lee, S. Y.; Kang, N. R.; Lee, Y. M.; Guiver, M. D. Fluorene-Based Poly(arylene ether sulfone)s Containing Clustered Flexible Pendant Sulfonic Acids as Proton Exchange Membranes. *Macromolecules* **2011**, *44*, 7296−7306.
(45) McKeen, J. C.; Yan, Y. S.; Davis, M. E. Proton Conductivity of Acid-Functionalized Zeolite Beta, MCM-41, and MCM-48: Effect of Acid Strength. *Chem. Mater.* **2008**, *20*, 5122−5124.
(46) Liu, W.; Wang, S.; Xiao, M.; Han, D.; Meng, Y. A Proton Exchange Membrane Fabricated from a Chemically Heterogeneous Nonwoven with Sandwich Structure by the Program-Controlled Co-Electrospinning Process. *Chem. Commun.* **2012**, *48*, 3415−3417.
(47) Ludueña, G. A.; Kühne, T. D.; Sebastiani, D. Mixed Grotthuss and Vehicle Transport Mechanism in Proton Conducting Polymers from ab Initio Molecular Dynamics Simulations. *Chem. Mater.* **2011**, *23*, 1424−1429.
(48) Zarrin, H.; Higgins, D.; Jun, Y.; Chen, Z.; Fowler, M. Functionalized Graphene Oxide Nanocomposite Membrane for Low Humidity and High Temperature Proton Exchange Membrane Fuel Cells. *J. Phys. Chem. C* **2011**, *115*, 20774−20781.
(49) Yao, Y.; Lin, Z.; Li, Y.; Alcoutlabi, M.; Hamouda, H.; Zhang, X. Superacidic Electrospun Fiber-Nafion Hybrid Proton Exchange Membranes. *Adv. Energy Mater.* **2011**, *1*, 1133−1140.